One-Pot Conversion of Furfural to γ-Valerolactone over Co- and Pt-Doped ZSM-5 Catalysts

Weerachon Tolek [1], Warucha Auppahad [1], Patcharaporn Weerachawanasak [2], Okorn Mekasuwandumrong [3], Piyasan Praserthdam [1] and Joongjai Panpranot [1,4,*]

[1] Center of Excellence on Catalysis and Catalytic Reaction Engineering, Department of Chemical Engineering, Faculty of Engineering, Chulalongkorn University, Bangkok 10330, Thailand

[2] Department of Chemistry, Faculty of Science, King Mongkut's Institute of Technology Ladkrabang, Bangkok 10520, Thailand

[3] Department of Chemical Engineering, Faculty of Engineering and Industrial Technology, Silpakorn University, Nakhon Pathom 73000, Thailand

[4] Bio-Circular-Green-Economy Technology & Engineering Center, BCGeTEC, Department of Chemical Engineering, Faculty of Engineering, Chulalongkorn University, Bangkok 10330, Thailand

* Correspondence: joongjai.p@chula.ac.th; Tel.: +66-2218-6869; Fax.: +66-2218-6877

Abstract: γ-Valerolactone (GVL) is one of the useful biomass compounds produced via different reaction pathways from hemicellulose. In this study, Co- and Pt-doped/ZSM-5 catalysts with different Co loadings (0–10 wt.%) and Pt loadings (0.5–2 wt.%) were prepared by impregnation method and employed in a one-pot conversion of furfural to GVL. The yield of GVL increased with increasing reaction temperature from 100 to 140 °C. At the reaction temperature of 120 °C, higher amounts of secondary products such as AL and IPL can be converted to GVL, especially on the Co- and Pt-modified ZSM-5 catalysts. Compared to the non-modified H-ZSM-5 (GVL yield 35.4%), Co- and Pt-doped ZSM-5 catalysts exhibited much higher yield of GVL with the 1%Pt/ZSM-5 catalyst showing the highest yield of GVL at 85.4% at 120 °C and 1 bar N_2 without the use of liquid acid or external H_2 supply. The catalyst performances were correlated to the physicochemical properties of the catalysts such as the amount and type of acid sites. The NH_3-TPD and in situ FTIR spectra of pyridine adsorption results revealed that Co- and Pt-loaded on ZSM-5 enhanced Lewis and weak acid sites, which are beneficial for the reaction. The results present a simple strategy to obtain high GVL yield under relatively mild conditions.

Keywords: one-pot conversion; furfural; furfuryl alcohol; γ-valerolactone; ZSM-5

1. Introduction

Reducing the use of fossil fuels that causes environmental problems through alternative energy is an important issue nowadays. Lignocellulosic biomass is considered as an alternative feedstock to produce sustainable energy because of its abundance and the neutralization of carbon [1]. Usually, lignocellulose biomass consists of cellulose, hemicellulose, and lignin. Xylose, derived from hemicellulose can be converted to furfural through a dehydration process with acid catalyst [2]. Recently, the conversion of furfural to higher valuable chemicals such as γ-valerolactone (GVL), levullinic acid (LA), isopropyl levulinate (IPL), angelica lactones (AL), and levullinate ester (LE) has received considerable attention [3,4]. GVL is an important chemical with a wide range of applications. It is used as a solvent for biomass-related reactions, fine chemical intermediates, and a building block for polymers and fuels [5–11].

The production of GVL from furfural involves multiple reaction steps which consist of the hydrogenation of furfural, the acid-catalyzed ring-opening of furfuryl alcohol (FA), and finally the hydrogenation of levulinic acid (LA) or its esters to GVL [11–13]. The application of the Meerwein–Ponndorf–Verley (MPV) reduction pathway to GVL production is the

way for the development of a one-pot process [14]. Instead of using high-pressure H_2, the transfer hydrogenation pathway, such as MPV reduction, enables the selective hydrogenation of LA or furfural to the corresponding products with metal or acid-base properties using secondary alcohols as a hydrogen donor [15–17]. Lewis and Brønsted acid sites are required to achieve the catalytic transfer of hydrogen (CTH) in a one-pot conversion of furfural to GVL. Finding well-balanced Lewis and Brønsted acids is of great significance in order to improve the catalytic performance. Therefore, one-pot conversion of furfural to give desired bio-products in high yields using a heterogeneous catalyst is particularly challenging. The production of GVL from furfural has been achieved by acid-catalyzed reaction using zeolite-based catalysts and also by catalytic transfer hydrogenation [18–23]. Zhu et al. [19] reported the formation of GVL from hemicellulose and furfural with alcohol solvent (IPA) over the combination of Au/ZrO_2 with ZSM-5. A GVL yield of 61.5% was mainly ascribed to the strong interface interaction of Au with ZrO_2 species, large amounts of medium-strength acid sites over ZSM-5, and efficient synergy between active metal and acid sites. According to previous studies [22–26], Co and Pt are promising hydrogenation metal due to their highly active to C=C and C=O bonds. Audemar et al. [23] studied the effect of reduction temperature, H_2 pressure and reaction temperature for selective hydrogenation of furfural to furfuryl alcohol. High selectivity (96%) at a conversion higher than 95% was reported over cobalt supported SBA-15 catalyst for optimum reaction conditions (150 °C, 1.5 h and 2.0 MPa of H_2). The conversion of furfural on zeolite-encapsulated Pt nanoparticles to valeric acid and ethyl valerate (VA/EV) via tandem reaction in one pot was reported to have achieved good yield of 86% [22]. However, the synthesis of GVL from furfural has not been realized, reflecting the characteristics of Co- and Pt-doped ZSM-5 and their structural-activity relationship in the development of catalysts for one-pot conversion.

In this work, one-pot conversion of furfural to GVL product was investigated using Co- and Pt-doped ZSM-5 catalysts under mild reaction conditions. The monometallic Co/ZSM-5 and Pt/ZSM-5 were prepared by incipient wetness impregnation method. The catalysts were characterized by various techniques such as BET, XRD, NH_3-TPD, and in situ FTIR spectra of pyridine adsorption. The catalysts functionalities were derived and correlated with their activity.

2. Experimental

2.1. Catalyst Preparation

The monometallic Co- (1–10 wt.%) and Pt- (0.5–2.0 wt.%) based catalysts were prepared by incipient wetness impregnation method using cobalt naphthenate ($CoC_{22}H_{14}O_4$, 6 wt.% in mineral spirits (Aldrich, Merck KGaA, Darmstadt, Germany) and platinum (II) acetylacetonate ($Pt(C_5H_7O_2)_2$, 99.99%, Aldrich) as Co and Pt precursors, respectively, on the H-ZSM-5 (Si/Al ratios of 15, Riogen, Mantua, NJ, USA) support. These catalysts are denoted as x%Co/ZSM-5 and x%Pt/ZSM-5, where x indicated to Co and Pt metal loadings, respectively. In a typical synthesis of 0.5%Pt/ZSM-5, 20 mg of $Pt(C_5H_7O_2)_2$ was dissolved in 2 mL of toluene, and then the Pt solution was added dropwise to the 2 g of H-ZSM-5. The catalyst was placed at room temperature for 2 h, dried in an oven at 100 °C overnight, and then calcined at 500 °C at ramp rate of 10 °C/min under an air flow of 100 cm^3/min for 2 h.

2.2. Catalyst Characterization

The BET (Brunauer–Emmett–Teller) surface area was performed with nitrogen as adsorbate at −196 °C after pre-treatment of the samples at 200 °C under nitrogen flow. For determination of the multi-point method surface area, the samples were examined from nitrogen adsorption by using Micrometrics Chemisorbs 2750. The pore structural data were analyzed by BJH (Barrett–Joyner–Halenda) method using Halsey equation for multilayer thickness. The total pore volume data were analyzed by BJH method cumulative desorption pore volume. X-ray diffraction analysis (XRD) was used to analyze the crystallinity and the structure of a catalyst. The refraction or diffraction of the X-rays was monitored at

various angles with respect to the primary beam X-ray diffraction analysis using an X-ray refractometer, SIEMENS XRD D5000, with Ni-filtered CuKα radiation in the 2θ range of 20° to 80° with step size of 0.02° and an acquisition time of 0.5 s per step. The acidic properties of the catalysts were analyzed using a Micromeritic Chemisorb 2750 apparatus. Prior to NH_3 adsorption, a 0.1 g sample was pretreated at 500 °C for 1 h under He flow (25 cm^3/min). After cooling to 40 °C, NH_3 was adsorbed using a flow of 15 vol % NH_3/He (20 cm^3/min) for 0.5 h. The NH_3 desorption was performed in He (20 cm^3/min) with a heating rate of 10 °C/min, and the NH_3 desorption profiles were registered with a thermal conductivity detector. In situ FTIR spectra of pyridine adsorption was used to determine the Brønsted and Lewis acid sites of the sample with a Bruker Equinox 55 FT-IR spectrometer having a mercury cadmium telluride (MTCB) detector. The 0.025g of wafer catalyst sample was preheated at 550 °C for 1 h with 10 °C/min in a vacuum. After that, the operating temperature was decreased to 40 °C to adsorb the pyridine for 10 min. The sample was evacuated at 40 °C for 1 h, and the IR spectra was recorded at 40 °C. The intensity of the Brønsted and Lewis acid sites in each sample was determined by the subtraction of the IR spectra after sample pretreatment from the IR spectra of sample evacuation at 40 °C for 1 h.

2.3. Catalytic Reaction Study

Prior to the reaction test, the catalyst was reduced with hydrogen (25 cm^3/min) at 500 °C for 2 h. Approximately 0.2 g of catalyst was dispersed into the reactant mixture of 0.5 mmol of furfural (99%, Aldrich) and 10 g of 2-propanol (98%, Aldrich) in 100 cm^3 high-pressure stainless steel autoclave reactor (JASCO, Tokyo, Japan) equipped with magnetic stirrer. The reactor was purged with N_2 two times to remove O_2 in the reactor and then pressurized with N_2 at 0.1 MPa. Then, the reactor was heated to 120 °C at a rate of 10 °C/min. To avoid mass and heat transfer barriers, stirring was set at 500 rpm when the reactor reached the desired temperature and maintained for 10 min before the reaction started. After 5 h of reaction time, the reaction was terminated by rapidly cooling the reactor using an ice-water bath to room temperature. When the temperature reached 25 °C, the gas in the reactor was purged into the atmosphere. After that, the liquid product was collected, and the solid catalyst was separated from the liquid product using a centrifuge at 5000 rpm for 5 min. In the last step, the liquid product was analyzed by a Shimadzu gas chromatograph equipped with a flame ionization detector (FID) and Rtx-5 capillary column (Restek, USA, 30 m × 0.25 mm ID, 0.25 μm). Typically, 2 μL of liquid product was injected into the column. The products were quantitatively analyzed by column calibration with corresponding standard chemicals. The furfural conversion, product selectivity, GVL yield, and carbon balance of the products were calculated using the GC-FID results and the following equations:

$$\text{Furfural conversion (\%)} = \left(\frac{\text{moles of initial furfural} - \text{moles of final furfural}}{\text{moles of initial furfural}} \right) \times 100, \quad (1)$$

$$\text{Product i selectivity (\%)} = \left(\frac{\text{moles of product i produced}}{\text{moles of initial furfural} - \text{moles of final furfural}} \right) \times 100, \quad (2)$$

$$\text{GVL yield (\%)} = \left(\frac{\text{moles of GVL produced}}{\text{moles of initial furfural}} \right) \times 100, \quad (3)$$

$$\text{Carbon balance (\%)} = \left(\frac{\text{moles of carbon of products detected}}{\text{moles of carbon of initial furfural}} \right) \times 100 \quad (4)$$

3. Results and Discussion

The XRD diffraction patterns of the Co- and Pt-based catalysts are shown in Figure 1. The XRD pattern of ZSM-5 is also presented in the same figure for comparison. The diffraction patterns corresponding to the ZSM-5 structure were still detected on the Co/ZSM-5 catalysts with 1, 5, and 10 wt.% of Co loading, but the peak intensity was gradually decreased. A significant loss of zeolite crystallinity was observed on the 10%Co/ZSM-5 with the appearance of new angles at 2θ = 21.0°, 31.8°, 36.0°, 38.6°, and 47.8°, which are assigned

to Co_3O_4 and the other peaks at $2\theta = 29.3°$, $42.4°$, and $56.7°$ which are assigned to cobalt silicate (Co_2SiO_4) species [27,28]. The Pt/ZSM-5 catalysts exhibited similar diffraction patterns of ZSM-5 with a slightly lower intensity compared to those of the Co/ZSM-5 catalysts. There were no differences in the crystalline patterns of ZSM-5 after Pt was added. The crystallinities of all the samples were calculated, and the values are presented in Table 1. For the calculations, the crystallinity of the ZSM-5 was taken as 100%. As expected, both Co- and Pt-based catalysts showed lower crystallinities than the undoped ZSM-5.
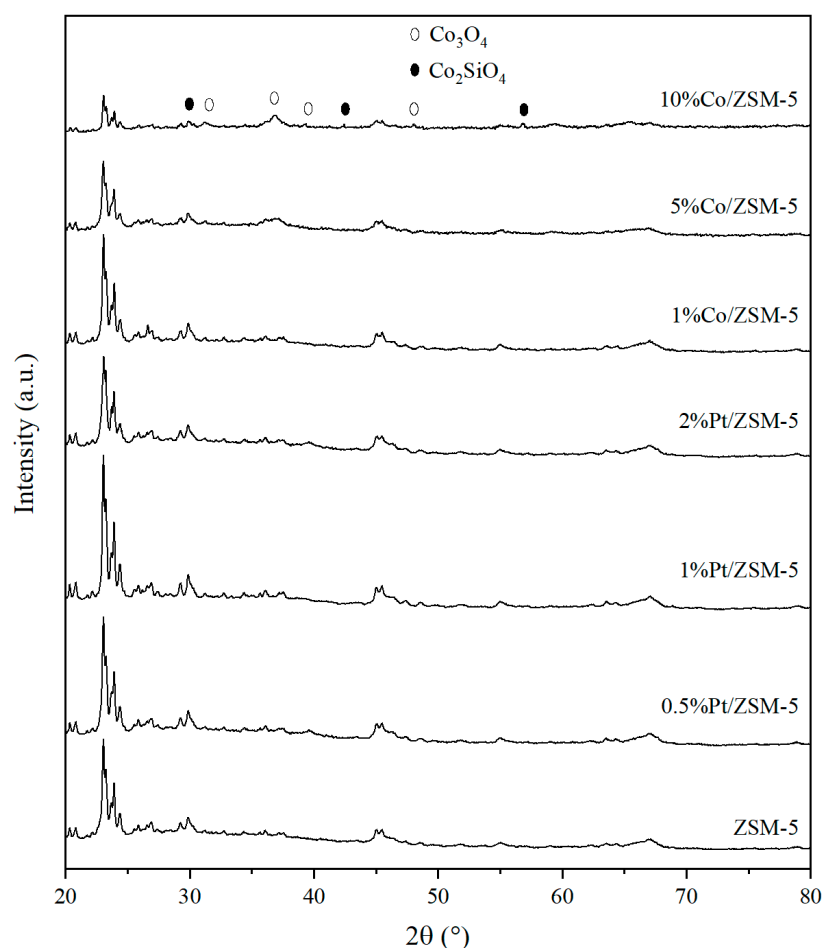

Figure 1. XRD patterns of the Co- and Pt-doped ZSM-5 catalysts.

Table 1. The crystallinity calculated from XRD results and textural properties of the Co- and Pt-doped ZSM-5 catalysts.

Catalysts	Crystallinity [a] (%)	BET Surface Area (m^2/g)	Average Pore Diameter [b] (nm)	Pore Volume [b] (cm^3/g)
10%Co/ZSM-5	32.2	207	1.52	0.23
5%Co/ZSM-5	45.3	217	1.87	0.24
1%Co/ZSM-5	78.1	227	1.92	0.25
2%Pt/ZSM-5	82.1	259	1.74	0.24
1%Pt/ZSM-5	85.5	280	1.95	0.24
0.5%Pt/ZSM-5	95.2	282	2.02	0.26
ZSM-5	100	292	2.11	0.26

[a] Base on XRD results. [b] Determined from the Barret–Joyner–Halenda (BJH) desorption method.

The catalyst textural properties were investigated by N_2 adsorption technique. The BET surface area, pore volume, and pore diameter of all the catalysts are shown in Table 1.

For the Co/ZSM-5 catalysts, the surface area and pore volume decreased with increasing Co loading. The decrease in BET surface area may occur due to blocking of certain zeolite pores by cobalt. On the contrary, the surface area and pore volume of the Pt/ZSM-5 catalysts did not change significantly with increasing Pt loading.

The acidic properties of the catalysts were investigated by NH_3-TPD and the results are displayed in Figure 2. The curves were deconvoluted into individual peaks by Gaussian deconvolution method, which are shown as dashed lines. All the catalysts showed a similar appearance consisting of two desorption peak regions at (I) 100–350 °C and (II) 350–550 °C. Based on other ZSM-5-based catalysts reported in the literature [29–31], these peaks could be inferred to be weak acid sites or physically adsorbed ammonia and strong acidic sites. A semi-quantitative comparison of the acid distribution was expressed as μmol NH_3/g of catalyst with respect to weak and strong acidic sites and summarized in Table 2. It was found that increasing Co loading led to an increase in weak acid sites, but strong acid sites decreased. The total acidity of Co/ZSM-5 catalysts decreased compared to ZSM-5 support. Lu et al. reported somewhat similar results for Co species insertion on Sn-beta zeolite that exhibited a slight decrease of the density of strong acid sites while the weak acid sites markedly increased [32]. In the same manner as Co-doped ZSM-5 catalysts, the increase of Pt loading also led to an increase in weak acid sites while strong acid sites decreased and the total acidity of Pt/ZSM-5 catalysts slightly decreased compared to the pristine ZSM-5. This phenomenon indicated the addition of Co and Pt on ZSM-5 catalyst was important to improve the proper acid properties which may have contributed to the conversion of FA to GVL.
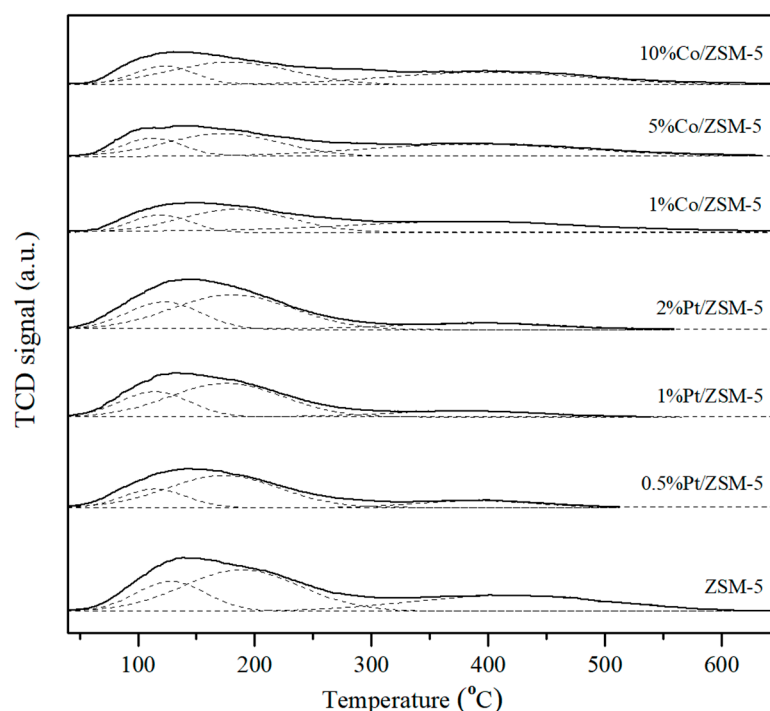

Figure 2. NH_3-profiles of the Co- and Pt-doped ZSM-5 catalysts. The deconvoluted peaks are shown as dashed lines.

The acid sites distribution of Lewis (L) and Brønsted (B) of the synthesized Co- and Pt-doped ZSM-5 catalysts were also identified by in situ FTIR spectra of pyridine adsorption, and the results are shown in Figure 3. Absorption bands at 1445 cm^{-1} were associated with pyridine adsorbed on Lewis acid sites. Absorption bands at 1546 cm^{-1} were associated with pyridine adsorbed on Brønsted acid sites, while the 1490 cm^{-1} was ascribed to pyridine absorbed on both Lewis and Brønsted acid sites or the hydrogen-bonded pyridine [33–37]. Table 2 summarizes the ratio (B/L) of Brønsted to Lewis acids of all the catalysts obtained

from the FTIR spectra of pyridine adsorption. It was found that the B/L ratio decreased as Co loading increased, indicating that higher Lewis acid sites correlate with increasing Co loading. When Pt metal was incorporated into the ZSM-5, the B/L ratio of the Pt/ZSM-5 catalysts also decreased, indicating that Lewis acid sites also markedly increased compared to bare ZSM-5. From the NH_3-TPD and pyridine-IR results, the density of weak and Lewis acid sites increased proportionately with an increase in Co and Pt loading on the ZSM-5 catalysts. This result suggested that the GVL yield was correlated to the different characteristics of the acidic properties. The proper B/L ratio would promote the GVL yield. In other words, Brønsted and Lewis acid sites in close proximity have a synergistic effect in catalyzing this cascade reaction [38].

Table 2. The acid properties of Co- and Pt-doped ZSM-5 catalysts.

Catalysts	Total Acidity [a] (μmol/g)	Weak Acidity [a] (μmol/g)	Strong Acidity [a] (μmol/g)	B/L Ratio [b]
10%Co/ZSM-5	832	454	378	0.16
5%Co/ZSM-5	821	466	355	0.12
1%Co/ZSM-5	802	460	342	0.48
2%Pt/ZSM-5	859	562	297	0.51
1%Pt/ZSM-5	844	547	297	0.66
0.5%Pt/ZSM-5	827	532	295	0.38
ZSM-5	862	324	538	1.21

[a] Determined by NH_3-TPD technique. [b] Determined by in-situ FTIR spectra of pyridine adsorption.

Catalytic Reaction Study

　　The catalytic activity and selectivity of ZSM-5 were investigated for furfural conversion at 100, 120, and 140 °C, 0.1 MPa with N_2 for 5 h. The reaction results are shown in Table 3. The conversion of furfural at 100 and 120 °C was 51.1% and 66.7% with 19.0% and 35.4% GVL yield, respectively. The increased reaction temperature to 140 °C resulted in the conversion to 75.1% with a yield of 53.3% GVL. The yield of the main product (GVL) increased with increasing reaction temperature. The results are in good agreement with those observed by Winoto et al. that furfural conversion and the yield of GVL were improved with the increase in reaction temperature from 120 to 180 °C [38]. However, the elevation of reaction temperature decreased in the main product GVL. The carbon balance of reaction temperature at 140 °C was relatively low, which may be caused by the instability of product at an elevated temperature, possibly by forming humins or polymers that cannot be detected by using GC [39,40]. According to a previous study by Rao et al. [18], a decrease in GVL yield was observed at a reaction temperature of 200 °C because of the formation of humin by-products. In our study, the optimum reaction temperature at 120 °C was an appropriate choice for further investigation on the effect of catalyst modification by Co- and Pt-doped ZSM-5 catalysts for the conversion of furfural to GVL.

　　The catalytic activity and selectivity of Co (1, 5 and 10 wt.%) loaded on ZSM-5 were investigated for furfural conversion at 120 °C, 0.1 MPa with N_2 for 5 h. The reaction results are shown in Table 4. Typically, ZSM-5 contains high amount of Brønsted acid with a B/L ratio of 1.21. Co-doped ZSM-5 catalysts showed an increase in weak and Lewis acid sites. The combination of Lewis acid and Brønsted acid is required for direct production of GVL from furfural [1]. The Co/ZSM-5 catalysts with an appropriate qualification can help conversion of the intermediate products (AL, LA and IPL) to GVL. Both furfural conversion, as well as GVL selectivity were markedly increased on the 1%Co/ZSM-5 catalyst, comparing to non-modified ZSM-5. The 1%Co/ZSM-5 catalyst presents the highest conversion and GVL selectivity at 68.0% and 86.0%, respectively. With further increase of Co loading to 10 wt.%, both conversion and selectivity of GVL dropped, due probably to the decrease in BET surface area at high Co loading. The high BET surface area of ZSM-5 may accommodate the diffusion of furfural and GVL. From the catalyst characterization catalysts, weak acidic sites was found to favor the formation of GVL,

which is in agreement with the results of Lu et al. [32]. For the Pt/ZSM-5 catalysts, both furfural conversion and GVL selectivity were markedly increased on the Pt/ZSM-5 catalyst, comparing to the non-modified ZSM-5 and the Co/ZSM-5. The high Brønsted acid sites of ZSM-5 catalyst may be necessary for the conversion of FA/FE to intermediate products such as AL or LA. The increase of weak and Lewis acid sites of the Pt/ZSM-5 catalysts was similar to the Co/ZSM-5 catalysts. Metal-catalyzed or Lewis acid sites promote furfural MPV reduction reaction to FA and LA hydrogenation toward GVL [23,32,41]. In the one-pot conversion of furfural to GVL, a suitable B/L ratio on 1%Pt/ZSM-5 catalyst (B/L ratio 0.66) demonstrated the highest conversion, GVL selectivity, and yield of 88.8%, 96.2%, and 85.4%, respectively. When Pt loading was increased to 2 wt.%, the BET surface area and B/L ratio decreased, resulting in lower catalytic activity than 1 wt.% of Pt loading.
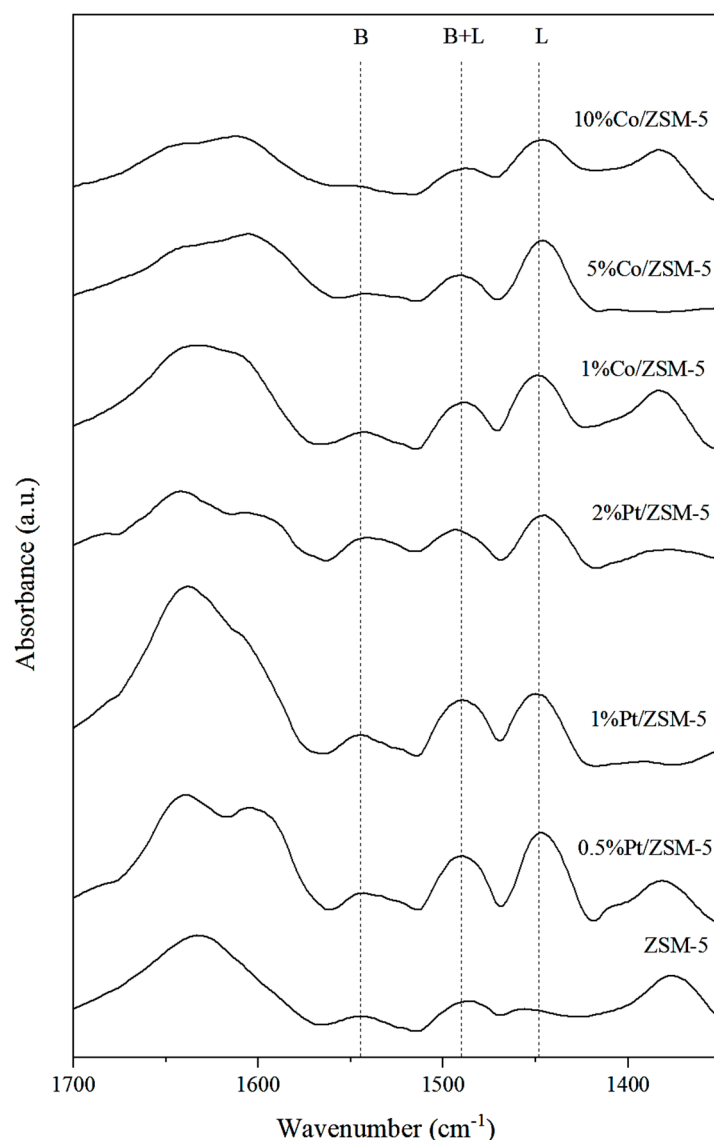

Figure 3. FT-IR spectra of pyridine adsorbed the Co- and Pt-doped ZSM-5 catalysts.

Table 3. Catalytic performances of furfural conversion to GVL over ZSM-5 catalyst with different reaction temperatures.

Temperature (°C)	Conversion (%)	Selectivity (%)				GVL Yield (%)	Carbon Balance (%)
		GVL	LA	AL	IPL		
100	51.1	25.3	64.1	6.30	4.30	19.0	100
120	66.7	53.1	4.00	20.3	22.6	35.4	100
140	75.1	71.0	4.60	3.20	3.50	53.3	82.3

Reaction conditions: 0.5 mmol of furfural in 10 g of 2-propanol under 0.1 MPa N_2 with 0.2 g catalyst for 5 h.

Table 4. Catalytic performances of furfural conversion to GVL over Co- and Pt-doped ZSM-5 catalysts to GVL under mild reaction conditions.

Catalysts	Conversion (%)	Selectivity (%)				GVL Yield (%)
		GVL	LA	AL	IPL	
10%Co/ZSM-5	44.6	53.8	27.1	15.7	3.5	24.0
5%Co/ZSM-5	53.4	59.3	22.8	13.9	4.0	31.7
1%Co/ZSM-5	68.0	86.0	3.7	5.7	4.6	58.5
2%Pt/ZSM-5	85.7	82.2	0	0	0	70.2
1%Pt/ZSM-5	88.8	96.2	0	0	0	85.4
0.5%Pt/ZSM-5	35.5	59.2	8.7	0	18.7	21.0
ZSM-5	66.7	53.1	4.0	20.3	22.6	35.4

Reaction conditions: 0.5 mmol of furfural in 10 g of 2-propanol at 120 °C under 0.1 MPa N_2 with 0.2 g catalyst for 5 h.

The reaction effects with time for the furfural conversion, as well as GVL selectivity were investigated. The furfural conversion, product selectivity, and yield of GVL as a function of reaction time over 1%Pt/ZSM-5 are shown in Table 5. At a reaction time of 2 h, furfural conversion (46.5%) was just started towards the 19.2% yield of GVL with LA and IPL selectivity of 3.2% and 23.1%, respectively. After 5 h of reaction, the conversion of furfural was promoted to 88.8% with 85.4% yield of GVL while the LA and IPL formations disappeared. The production rates and TOF of 1%Pt/ZSM-5 catalyst were 0.09 mmol/h and 1.05 h^{-1} at 5 h of reaction, respectively. The furfural conversion increased with increasing time and reached to the highest conversion at 10 h with 87.8% of GVL yield.

Table 5. Catalytic performances of furfural conversion to GVL over 1%Pt/ZSM-5 catalyst with various reaction times.

Reaction Time (h)	Conversion (%)	Selectivity (%)				GVL Yield (%)
		GVL	LA	AL	IPL	
2	46.5	41.2	3.2	0	23.1	19.2
5	88.8	96.2	0	0	0	85.4
10	95.7	91.7	0	0	0	87.8

Reaction conditions: 0.5 mmol of furfural in 10 g of 2-propanol at 120 °C under 0.1 MPa N_2 with 0.2 g catalyst.

The reusability test was performed on the 1%Pt/ZSM-5 due to its superior performance, and the results are summarized in Table 6. To explore the reusability performance, the used 1%Pt/ZSM-5 catalyst was separated by high-speed centrifugation after the reaction, repeatedly washed with 2-propanol, and dried at 100 °C. Prior to the next reaction test, the recovered catalyst was reduced under hydrogen (25 cm^3/min) at 500 °C with a ramp rate of 10 °C/min for 2 h. The activated catalyst was reused under the same reaction conditions for the next three consecutive runs. The GVL yield remained almost unchanged at 83–85% during the four cycles of run, indicating the high stability and reusability of the 1%Pt/ZSM-5 catalyst. The slight deactivation was probably due to the adsorption of intermediate compounds, which may block the pore or active sites.

Table 6. Reusability test of furfural conversion to GVL over 1%Pt/ZSM-5 catalyst.

Reaction Cycles	Conversion (%)	Selectivity (%)				GVL Yield (%)
		GVL	LA	AL	IPL	
1	88.8	96.2	0	0	0	85.4
2	88.0	95.8	0	0	0	84.3
3	87.8	95.6	0	0	0	83.9
4	87.7	94.3	0	0	0	82.7

Many catalysts have been used for GVL production via MPV using various primary and secondary alcohols including transition metal oxides, zeolites, and other noble and non-noble-metal catalysts [42,43]. It has been shown that Lewis acidic or metal catalysts such as Pt are effective in GVL production from LA/ levulinate ester. However, the presence of Brønsted acid sites is also necessary when starting from furfural. In order to convert furfural to GVL in a one-pot process, it is therefore highly desirable to develop an efficient multifunctional heterogeneous catalyst. Based on the previous reports [1,12,38,44–48], a possible reaction network scheme for the one-pot conversion of furfural to GVL over the multifunctional catalysts (Lewis/Brønsted acid and metal sites) is depicted in Figure 4. It can be seen that the multiple-step reaction was required to complete the conversion of furfural to GVL by using acid and metal catalyzed reaction. Lewis acid or metal-catalyzed reaction promoted furfural Meerwein–Ponndorf–Verley (MPV) reduction into furfuryl alcohol (FA) via selective hydrogenation of C = O bond of an aldehyde group using 2-propanol as a hydrogen donor. Subsequently, etherification was achieved to form furfuryl ether (FE). Hydrolysis and alcoholysis were catalyzed by Brønsted acid of FE with 2-propanol to LA/IPL or AL. Catalyzed by Lewis acid or metal-catalyzed MPV reaction, the Isopropyl levulinate (IPL) was reduced to Isopropyl 4-hydroxypentanoates, followed by lactonization to form γ-valerolactone (GVL).
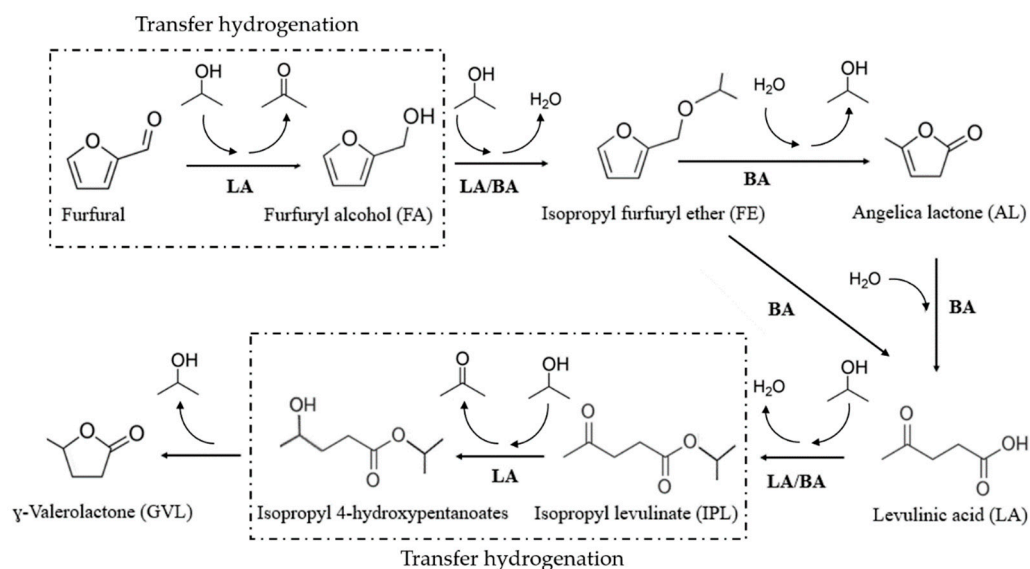

Figure 4. Reaction networks for the one-pot conversion of furfural to GVL (BA: Brønsted acid, LA: Lewis acid). Reaction conditions: 0.5 mmol of furfural in 10 g of 2-propanol at 120 °C under 0.1 MPa N_2 with 0.2 g catalyst.

4. Conclusions

One-pot synthesis of GVL from furfural was studied over Co- and Pt-doped ZSM-5 catalysts. The yield of the main product (GVL) increased with increasing reaction temperature from 100 to 140 °C. At a lower reaction temperature of 100 °C, mostly the reaction reached the stage of LA formation with small amount of GVL. At the reaction temperature

of 120 °C, higher amounts of secondary products such as AL, IPL could be converted to GVL, especially on the Co- and Pt-modified ZSM-5 catalysts. From the NH_3-TPD and the pyridine-IR results, Co- and Pt-loaded on ZSM-5 increased Lewis and weak acid sites, which are beneficial for the reaction. The appropriate acid properties and metal-catalyzed pathway facilitated MPV reduction of furfural to γ-Valerolactone (GVL). The 1%Pt/ZSM-5 catalyst presents the highest conversion of 88.8% and GVL selectivity of 96.2% under 120 °C, 0.1 MPa with N_2 for 5 h. The production rates and TOF of 1%Pt/ZSM-5 catalyst were 0.09 mmol/h and 1.05 h^{-1}, respectively. A 85.4% yield of GVL was obtained from furfural conversion. This provides a facile route to synthesize GVL under mild conditions without using liquid acid and/or external H_2 supply.

References

1. Winoto, H.P.; Fikri, Z.A.; Ha, J.-M.; Park, Y.-K.; Lee, H.; Suh, D.J.; Jae, J. Heteropolyacid supported on Zr-Beta zeolite as an active catalyst for one-pot transformation of furfural to γ-valerolactone. *Appl. Catal. B Environ.* **2019**, *241*, 588–597. [CrossRef]
2. Bhogeswararao, S.; Srinivas, D. Catalytic conversion of furfural to industrial chemicals over supported Pt and Pd catalysts. *J. Catal.* **2015**, *327*, 65–77. [CrossRef]
3. Kim, J.; Byun, J.; Ahn, Y.; Han, J. Catalytic Production of Gamma-Valerolactone from Two Different Feedstocks. In *13th International Symposium on Process Systems Engineering (PSE 2018)*; Elsevier: Amsterdam, The Netherlands, 2018; pp. 295–300.
4. Yu, Z.; Lu, X.; Liu, C.; Han, Y.; Ji, N. Synthesis of γ-valerolactone from different biomass-derived feedstocks: Recent advances on reaction mechanisms and catalytic systems. *Renew. Sustain. Energy Rev.* **2019**, *112*, 140–157. [CrossRef]
5. Li, H.; Fang, Z.; Yang, S. Direct Catalytic Transformation of Biomass Derivatives into Biofuel Component γ-Valerolactone with Magnetic Nickel–Zirconium Nanoparticles. *ChemPlusChem* **2016**, *81*, 135–142. [CrossRef] [PubMed]
6. Cao, W.; Luo, W.; Ge, H.; Su, Y.; Wang, A.; Zhang, T. UiO-66 derived Ru/ZrO2@C as a highly stable catalyst for hydrogenation of levulinic acid to γ-valerolactone. *Green Chem.* **2017**, *19*, 2201–2211. [CrossRef]
7. Chen, C.-B.; Chen, M.-Y.; Zada, B.; Ma, Y.-J.; Yan, L.; Xu, Q.; Li, W.-Z.; Guo, Q.-X.; Fu, Y. Effective conversion of biomass-derived ethyl levulinate into γ-valerolactone over commercial zeolite supported Pt catalysts. *RSC Adv.* **2016**, *6*, 112477–112485. [CrossRef]
8. Yan, K.; Yang, Y.; Chai, J.; Lu, Y. Catalytic reactions of gamma-valerolactone: A platform to fuels and value-added chemicals. *Appl. Catal. B Environ.* **2015**, *179*, 292–304. [CrossRef]
9. Alonso, D.M.; Bond, J.Q.; Dumesic, J.A. Catalytic conversion of biomass to biofuels. *Green Chem.* **2010**, *12*, 1493–1513.
10. Bond, J.Q.; Upadhye, A.A.; Olcay, H.; Tompsett, G.A.; Jae, J.; Xing, R.; Alonso, D.M.; Wang, D.; Zhang, T.; Kumar, R.; et al. Production of renewable jet fuel range alkanes and commodity chemicals from integrated catalytic processing of biomass. *Energy Environ. Sci.* **2014**, *7*, 1500–1523. [CrossRef]
11. Alonso, D.M.; Wettstein, S.G.; Dumesic, J.A. Gamma-valerolactone, a sustainable platform molecule derived from lignocellulosic biomass. *Green Chem.* **2013**, *15*, 584–595. [CrossRef]
12. Bui, L.; Luo, H.; Gunther, W.; Román-Leshkov, Y. Domino reaction catalyzed by zeolites with Bronsted and Lewis acid sites for the production of gamma-valerolactone from furfural. *Angew. Chem. Int. Ed. Engl.* **2013**, *52*, 8022–8025. [CrossRef] [PubMed]
13. Li, F.; France, L.J.; Cai, Z.; Li, Y.; Liu, S.; Lou, H.; Long, J.; Li, X. Catalytic transfer hydrogenation of butyl levulinate to γ-valerolactone over zirconium phosphates with adjustable Lewis and Brønsted acid sites. *Appl. Catal. B Environ.* **2017**, *214*, 67–77. [CrossRef]
14. Gilkey, M.J.; Xu, B. Heterogeneous Catalytic Transfer Hydrogenation as an Effective Pathway in Biomass Upgrading. *ACS Catal.* **2016**, *6*, 1420–1436. [CrossRef]

15. Chia, M.; Dumesic, J.A. Liquid-phase catalytic transfer hydrogenation and cyclization of levulinic acid and its esters to γ-valerolactone over metal oxide catalysts. *Chem. Commun.* **2011**, *47*, 12233–12235. [CrossRef]

16. Song, J.; Wu, L.; Zhou, B.; Zhou, H.; Fan, H.; Yang, Y.; Meng, Q.; Han, B. A new porous Zr-containing catalyst with a phenate group: An efficient catalyst for the catalytic transfer hydrogenation of ethyl levulinate to γ-valerolactone. *Green Chem.* **2015**, *17*, 1626–1632. [CrossRef]

17. Koehle, M.; Lobo, R.F. Lewis acidic zeolite Beta catalyst for the Meerwein–Ponndorf–Verley reduction of furfural. *Catal. Sci. Technol.* **2016**, *6*, 3018–3026. [CrossRef]

18. Rao, B.S.; Kumari, P.K.; Koley, P.; Tardio, J.; Lingaiah, N. One pot selective conversion of furfural to γ-valerolactone over zirconia containing heteropoly tungstate supported on β-zeolite catalyst. *Mol. Catal.* **2019**, *466*, 52–59.

19. Zhu, S.; Xue, Y.; Guo, J.; Cen, Y.; Wang, J.; Fan, W. Integrated Conversion of Hemicellulose and Furfural into γ-Valerolactone over Au/ZrO2 Catalyst Combined with ZSM-5. *ACS Catal.* **2016**, *6*, 2035–2042. [CrossRef]

20. Zhang, H.; Yang, W.; Roslan, I.I.; Jaenicke, S.; Chuah, G.-K. A combo Zr-HY and Al-HY zeolite catalysts for the one-pot cascade transformation of biomass-derived furfural to γ-valerolactone. *J. Catal.* **2019**, *375*, 56–67. [CrossRef]

21. Song, S.; Di, L.; Wu, G.; Dai, W.; Guan, N.; Li, L. Meso-Zr-Al-beta zeolite as a robust catalyst for cascade reactions in biomass valorization. *Appl. Catal. B Environ.* **2017**, *205*, 393–403. [CrossRef]

22. Cho, H.J.; Kim, D.; Li, S.; Su, D.; Ma, D.; Xu, B. Molecular-Level Proximity of Metal and Acid Sites in Zeolite-Encapsulated Pt Nanoparticles for Selective Multistep Tandem Catalysis. *ACS Catal.* **2020**, *10*, 3340–3348. [CrossRef]

23. Audemar, M.; Ciotonea, C.; De Oliveira Vigier, K.; Royer, S.; Ungureanu, A.; Dragoi, B.; Dumitriu, E.; Jérôme, F. Selective Hydrogenation of Furfural to Furfuryl Alcohol in the Presence of a Recyclable Cobalt/SBA-15 Catalyst. *ChemSusChem* **2015**, *8*, 1885–1891. [CrossRef]

24. Zhang, G.; Vasudevan, K.V.; Scott, B.L.; Hanson, S.K. Understanding the mechanisms of cobalt-catalyzed hydrogenation and dehydrogenation reactions. *J. Am. Chem. Soc.* **2013**, *135*, 8668–8681. [CrossRef] [PubMed]

25. Liu, X.; Xu, L.; Xu, G.; Jia, W.; Ma, Y.; Zhang, Y. Selective Hydrodeoxygenation of Lignin-Derived Phenols to Cyclohexanols or Cyclohexanes over Magnetic CoNx@NC Catalysts under Mild Conditions. *ACS Catal.* **2016**, *6*, 7611–7620. [CrossRef]

26. Ohta, H.; Kobayashi, H.; Hara, K.; Fukuoka, A. Hydrodeoxygenation of phenols as lignin models under acid-free conditions with carbon-supported platinum catalysts. *Chem. Commun.* **2011**, *47*, 12209–12211. [CrossRef] [PubMed]

27. Valero-Romero, M.J.; Sartipi, S.; Sun, X.; Rodríguez-Mirasol, J.; Cordero, T.; Kapteijn, F.; Gascon, J. Carbon/H-ZSM-5 composites as supports for bi-functional Fischer–Tropsch synthesis catalysts. *Catal. Sci. Technol.* **2016**, *6*, 2633–2646. [CrossRef]

28. El-Bahy, Z.M.; Mohamed, M.M.; Zidan, F.I.; Thabet, M.S. Photo-degradation of acid green dye over Co-ZSM-5 catalysts prepared by incipient wetness impregnation technique. *J. Hazard. Mater.* **2008**, *153*, 364–371. [CrossRef] [PubMed]

29. Cheon, J.-Y.; Kang, S.-H.; Bae, J.W.; Park, S.-J.; Jun, K.-W.; Dhar, G.M.; Lee, K.-Y. Effect of Active Component Contents to Catalytic Performance on Fe-Cu-K/ZSM5 Fischer-Tropsch Catalyst. *Catal. Lett.* **2010**, *134*, 233–241. [CrossRef]

30. Kang, S.-H.; Ryu, J.-H.; Kim, J.-H.; Prasad, P.S.S.; Bae, J.W.; Cheon, J.-Y.; Jun, K.-W. ZSM-5 Supported Cobalt Catalyst for the Direct Production of Gasoline Range Hydrocarbons by Fischer–Tropsch Synthesis. *Catal. Lett.* **2011**, *141*, 1464. [CrossRef]

31. Lónyi, F.; Valyon, J. On the interpretation of the NH3-TPD patterns of H-ZSM-5 and H-mordenite. *Microporous Mesoporous Mater.* **2001**, *47*, 293–301. [CrossRef]

32. Lu, Y.; Li, W.; Zhu, Y.; Zhang, T.; Zhang, Q.; Liu, Q. One-pot Synthesis of High Value-added Chemicals from Furfural over Bimetal-doped Beta Zeolite and Carbon Solid Acid Catalysts. *Bioresources* **2018**, *13*, 5925–5941. [CrossRef]

33. Zaki, M.I.; Hasan, M.A.; Al-Sagheer, F.A.; Pasupulety, L. In situ FTIR spectra of pyridine adsorbed on SiO2-Al2O3, TiO2, ZrO2 and CeO2: General considerations for the identification of acid sites on surfaces of finely divided metal oxides. *Colloids Surf. A Physicochem. Eng. Asp.* **2001**, *190*, 261–274. [CrossRef]

34. Sasidharan, M.; Hegde, S.G.; Kumar, R. Surface acidity of Al-, Ga- and Fe-silicate analogues of zeolite NCL-1 characterized by FTIR, TPD (NH3) and catalytic methods. *Microporous Mesoporous Mater.* **1998**, *24*, 59–67. [CrossRef]

35. Poncelet, G.; Dubru, M.L. An infrared study of the surface acidity of germanic near-faujasite zeolite by pyridine adsorption. *J. Catal.* **1978**, *52*, 321–331. [CrossRef]

36. Auepattana-Aumrung, C.; Suriye, K.; Jongsomjit, B.; Panpranot, J.; Praserthdam, P. Inhibition effect of Na+ form in ZSM-5 zeolite on hydrogen transfer reaction via 1-butene cracking. *Catal. Today* **2020**, *358*, 237–245. [CrossRef]

37. Cui, R.; Ma, S.; Yang, B.; Li, S.; Li, J.; Pei, T.; Wang, J.; Sun, S.; Mi, C. The roles of Bronsted acidity in low-temperature catalytic oxidation of NO over acidic zeolites with H2O2. *Chemosphere* **2020**, *251*, 126561. [CrossRef] [PubMed]

38. Winoto, H.P.; Ahn, B.S.; Jae, J. Production of γ-valerolactone from furfural by a single-step process using Sn-Al-Beta zeolites: Optimizing the catalyst acid properties and process conditions. *J. Ind. Eng. Chem.* **2016**, *40*, 62–71. [CrossRef]

39. Ahmad, E.; Alam, I.; Pant, K.K.; Haider, M.A. Catalytic and mechanistic insights into the production of ethyl levulinate from biorenewable feedstocks. *Green Chem.* **2016**, *18*, 4804–4823. [CrossRef]

40. Chang, X.; Liu, A.-F.; Cai, B.; Luo, J.-Y.; Pan, H.; Huang, Y.-B. Catalytic Transfer Hydrogenation of Furfural to 2-Methylfuran and 2-Methyltetrahydrofuran over Bimetallic Copper-Palladium Catalysts. *ChemSusChem* **2016**, *9*, 3330–3337. [CrossRef]

41. Chen, X.; Zhang, L.; Zhang, B.; Guo, X.; Mu, X. Highly selective hydrogenation of furfural to furfuryl alcohol over Pt nanoparticles supported on g-C3N4 nanosheets catalysts in water. *Sci. Rep.* **2016**, *6*, 28558.

42. Osatiashtiani, A.; Lee, A.F.; Wilson, K. Recent advances in the production of γ-valerolactone from biomass-derived feedstocks via heterogeneous catalytic transfer hydrogenation. *J. Chem. Technol. Biotechnol.* **2017**, *92*, 1125–1135. [CrossRef]

43. Kobayashi, H.; Matsuhashi, H.; Komanoya, T.; Hara, K.; Fukuoka, A. Transfer hydrogenation of cellulose to sugar alcohols over supported ruthenium catalysts. *Chem. Commun.* **2011**, *47*, 2366–2368. [CrossRef] [PubMed]

44. Wang, T.; He, J.; Zhang, Y. Production of γ-Valerolactone from One-Pot Transformation of Biomass-Derived Carbohydrates Over Chitosan-Supported Ruthenium Catalyst Combined with Zeolite ZSM-5. *Eur. J. Org. Chem.* **2020**, *2020*, 1611–1619. [CrossRef]

45. Yuan, M.; Long, Y.; Yang, J.; Hu, X.; Xu, D.; Zhu, Y.; Dong, Z. Biomass Sucrose-Derived Cobalt@Nitrogen-Doped Carbon for Catalytic Transfer Hydrogenation of Nitroarenes with Formic Acid. *ChemSusChem* **2018**, *11*, 4156–4165. [CrossRef] [PubMed]

46. Guo, H.; Gao, R.; Sun, M.; Guo, H.; Wang, B.; Chen, L. Cobalt Entrapped in N,S-Codoped Porous Carbon: Catalysts for Transfer Hydrogenation with Formic Acid. *ChemSusChem* **2019**, *12*, 487–494. [CrossRef] [PubMed]

47. Roman-Leshkov, Y.; Moliner, M.; Labinger, J.A.; Davis, M.E. Mechanism of glucose isomerization using a solid Lewis acid catalyst in water. *Angew. Chem. Int. Ed. Engl.* **2010**, *49*, 8954–8957. [CrossRef] [PubMed]

48. Holm, M.S.; Pagán-Torres, Y.J.; Saravanamurugan, S.; Riisager, A.; Dumesic, J.A.; Taarning, E. Sn-Beta catalysed conversion of hemicellulosic sugars. *Green Chem.* **2012**, *14*, 702–706. [CrossRef]